Colloid Polym Sci
DOI 10.1007/s00396-013-2978-x

ORIGINAL CONTRIBUTION

Multistimuli-responsive hydrogels of poly (2-acrylamido-2-methyl-1-propanesulfonic acid) containing graphene

Valeria Alzari · Daniele Nuvoli · Roberta Sanna · Laura Peponi · Massimo Piccinini · Silvia Bittolo Bon · Salvatore Marceddu · Luca Valentini · Jose Maria Kenny · Alberto Mariani

Received: 7 February 2013 / Revised: 27 March 2013 / Accepted: 30 April 2013

Abstract Nanocomposite hydrogels of poly(2-acrylamido-2-methyl-1-propanesulfonic acid) containing graphene were prepared by radical polymerization. Their swelling properties in response to ionic strength and electrical stimuli were assessed. Graphene was obtained through an easy and convenient method lately developed by our research group, which consists in the exfoliation of graphite by sonicating it in a proper solvent medium. It was found that the graphene content influences the swelling properties of hydrogels; in particular, those containing graphene swell more than the filler-free ones; graphene content influences also the swelling ratio variation between the swollen and deswollen states.

Keywords Hydrogels · Nanocomposites · Polyelectrolytes · Stimuli-sensitive polymers · Swelling

V. Alzari · D. Nuvoli · R. Sanna · A. Mariani (✉)
Dipartimento di Chimica e Farmacia, Università degli Studi di Sassari e Unità locale INSTM, Via Vienna 2, 07100 Sassari, Italy
e-mail: mariani@uniss.it

L. Peponi · J. M. Kenny
Institute of Polymer Science and Technology (ICTP-CSIC), Calle Juan de la Cierva 3, 28006 Madrid, Spain

M. Piccinini
Porto Conte Ricerche S.r.l., SP 55 km 8.400 Loc., Tramariglio 07041 Alghero (SS), Italy

S. B. Bon · L. Valentini
Civil and Environmental Engineering Department, INSTM Research Unit, University of Perugia, Strada di Pentima 4, 05100 Terni, Italy

S. Marceddu
Consiglio Nazionale delle Ricerche (CNR), Istituto di Scienze delle Produzioni Alimentari (ISPA), Li Punti (Reg. Baldinca)Traversa La Crucca, 07100 Sassari, Italy

Introduction

Hydrogels containing a sulfonic acid group are a class of strong polyelectrolyte materials having a high degree of ionization. In particular, poly(2-acrylamido-2-methyl-1-propanesulfonic acid) (pAMPSA) is a superabsorbent hydrogel that exhibits an extensive coil-type expansion in aqueous solutions [1]. Moreover, it is a stimuli-responsive polymer [2] that changes its size and shape in response to variation of pH, ionic strength, and electrical field [3–5]. pAMPSA can be used in electrical and biochemical applications [6–8] and in the removal of heavy metal ions from water [9].

Electro-sensitive hydrogels, which are basically pH-sensitive materials, are able to convert chemical energy to mechanical one [10]. These systems can serve as actuators or artificial muscles in many applications [11]. Also, they have been applied in controlled drug delivery [12, 13]; for example, hydrogels made of poly(AMPSA-*co*-*n*-butylmethacrylate) were able to release edrophonium chloride and hydrocortisone in pulsatile manner using electric current [14].

pAMPSA hydrogel nanocomposites containing bio-modified montmorillonite were synthesized and studied by Kabiri et al. for the first time [15]. However, polymer composites based on pAMPSA have not been studied vastly yet.

Recently, nanocomposite hydrogels have attracted great interest thanks to the possibility to improve their properties

Published online: 05 July 2013

by using properly chosen nanofillers [16]; for example, nanocomposite hydrogels of poly(*N*-isopropylacrylamide) containing partially exfoliated graphite [17] or graphene [18] were synthesized by our research group.

Graphene has been chosen as a suitable filler thanks to its exceptional properties, namely, its high values of electrical conductivity [19], mobility of charge carriers (2×105 cm^2 V^{-1} s^{-1}) [20], and specific surface area (2,630 m^2 g^{-1}) [21]. High Young's modulus (≈1,100 GPa) [22], fracture strength (125 GPa) [22], and thermal conductivity (5×103 W m^{-1} K^{-1}) [19] are other exceptional properties. It is a two-dimensional layer consisting of sp^2 hybridized carbon atoms, which are densely packed in a honeycomb crystal lattice. Its peculiar lattice symmetry leads the excellent electronic properties; the unaffected p orbital, which is perpendicular to the planar structure, leads to the formation of a delocalized π bond.

The aim of this work was to study the stimuli-responsive properties of pAMPSA hydrogels under the effect of variation of ionic strength and electrical external field and the influence of graphene addition on polymeric matrix. This strategy allows obtaining stimuli-responsive nanocomposite hydrogels with different properties with respect to the filler-free ones.

To make them, graphene was obtained using a method improved recently by our research group [17, 18, 23–26], reported first by Hernandez et al. [27], consisting in the exfoliation of graphite in a liquid medium to form single- or few-layer graphene. In particular, we have obtained graphene in dimethyl sulfoxide [17], NMP [18], an ionic liquid [23], and in various reactive media, such as diisocyanates and diol [24], tetraethylene glycol diacrylate [25], vinylcaprolactam [26]; in addition, a novel and simple method to obtain "in situ" formed graphene/monomer dispersions and graphene/polymer nanocomposites was proposed [23–26].

In this work, we obtained graphene in dimethylformamide (DMF), a good solvent of the monomer, and the mixture of AMPSA and the graphene dispersion were radically polymerized to obtain the nanocomposite hydrogels.

Experimental section

Materials

AMPSA, molecular weight (MW): 207.25, d: 1.1 g/cm^3), dimethylformamide (DMF, MW: 73.08, b.p.: 152-154 °C), *N*,*N*′-methylene-bis-acrylamide (BIS, MW: 154.17) and graphite flakes were purchased by Sigma-Aldrich and used as received. Trihexyltetradecylphosphonium persulfate (TETDPPS, MW: 1,159) was used as the radical initiator and synthesized according to the method described in the literature [28].

Graphene stock dispersion in DMF

Graphite (5.0 g) dispersed in 100 g of DMF was introduced in a 250-mL flask; the mixture was sonicated in an ultrasonic bath at room temperature for 24 h. Then, the dispersion was centrifuged for 30 min at 4,000 rpm, and the residual solid graphite was removed. The concentration, calculated by gravimetry after filtration through polyvinylidene fluoride filters (pore size 0.22 μm), was found to be equal to 0.35 mg/mL.

Synthesis of pAMPSA hydrogels

In order to prepare hydrogels containing various amounts of graphene, the above stock dispersion was properly diluted with suitable amounts of DMF, and the resulting actual graphene concentrations were determined by UV–vis spectroscopy. The desired quantities of AMPSA were added to the obtained graphene dispersion, and the new resulting mixture was sonicated for 15 min. Then, the cross-linker (BIS, 5 mol% with respect to the molar concentration of AMPSA) and the initiator (TETDPPS, 0.5 mol% with respect to the molar concentration of AMPSA) were added. The investigated formulations are listed in Table 1.

A common test tube (inner diameter=1.5 cm, length=16 cm) was filled with the reacting mixture (Table 1). The polymerization was performed by keeping the tube immersed in an oil bath at 80 °C for 1 h.

Graphene/DMF dispersion characterization

The graphene stock dispersion in DMF was analyzed by UV–vis spectroscopy using the Hitachi U-2010 spectrometer (1 mm cuvette), following the method described in the literature [29]. Namely, a calibration line for graphene concentration was used (wavelength was 660 nm). The calculated absorption coefficient was 2,498 mL mg^{-1} m^{-1}. This was used to determine the actual graphene concentrations in any diluted dispersion derived from the stock one.

TEM measurements were performed on the JEOL JEM-2100 TEM instrument (JEOL Ltd., Akishima, Tokyo, Japan), with the LaB6 filament, with an operating voltage of 200 kV.

Table 1 Amount of graphene present in each nanocomposite hydrogel

Sample	Graphene content (wt% respect to monomer weight)
97.4	0.06
97.5	0.02
97.6	0.01
97.8	0

For TEM analysis, the solutions have been cast directly on the 200-mesh cooper grid and followed by solvent evaporation at ambient conditions for 24 h.

Raman analysis was performed with a Bruker Senterra Raman microscope, using an excitation wavelength of 532 nm at 5 mW. The spectra were acquired by averaging five acquisitions of 5 s with a ×50 objective.

Hydrogel samples characterization

After freeze-drying, the hydrogels were analyzed by SEM using the ZEISS DSM 962 CSEM scanning electron microscope. Prior to examination, all samples were fractured in liquid nitrogen, and the fractured surface was coated with gold.

To determine the swelling ratio (SR%) as a function of the ionic strength, the hydrogels were immersed in aqueous solutions of KNO_3 and $Ca(NO_3)_2$, to evaluate the influence of the type of cation. In particular, the ionic strength was varied from 0 to 0.1, and the pH was kept constant at 3; when the equilibrium was attained, the samples were weighed, and the SR% was calculated applying the following equation:

$$\mathrm{SR\%} = \frac{M_s - M_d}{M_d} \cdot 100 \quad (1)$$

where M_s and M_d are the hydrogel masses in the swollen and dry states, respectively.

To determine the SR% as a function of the variation of an electrical stimulus, the hydrogels were immersed in deionized water for 2 h. Then, they were cut into rectangular shaped blocks (10×10×5 mm). After precise weighing, each hydrogel sample was placed between the two metal electrodes. Since during the measurement the hydrogels deswell, the electrodes were forced to remain in contact with the sample during the whole experiment duration. The voltage applied was constant at 5, 15, or 30 V and applied for 30 s. Finally, the samples were weighed at the end of each test.

The relative weight change (RWC) due to the variation of the electrical field was calculated by the following equation:

$$\mathrm{RWC} = 1 - \left(\frac{M_i - M_f}{M_i}\right) \quad (2)$$

where M_f is the weight of the sample after treatment with the electric field, and M_i is the weight of the sample before treatment (conventionally, the weight of the sample not subjected to the electric field is equal to 1).

Results and discussion

Dispersion characterization

Graphene dispersion in DMF was analyzed by UV spectroscopy; in particular, the absorbance at different graphene concentrations was registered, and the calibration curve of the dispersion was obtained (Fig. 1). The system exhibits Lambert–Beer behavior, with an absorption coefficient of 2,498 mL mg^{-1} m^{-1} and a concentration of graphene, calculated by gravimetry, equal to 0.35 mg mL^{-1}.

Raman spectroscopy is a very powerful method for the characterization of single- and few-layer graphene. In particular, it allows an unambiguous distinction among single layer, bilayer, and multilayer [30]. This is possible through a comparison of the relative intensity of the characteristics G peak (at ~1,580 cm^{-1}) and 2D peak (at ~2,680 cm^{-1}) and by the symmetry of the 2D peak in the Raman spectra. The Raman spectrum of graphene obtained by filtration of its dispersion in DMF, compared with that of graphite (Fig. 2), shows that the 2D peak of graphite is made of two components; by contrast, the peak of graphene is symmetric, and its shape and position suggest that the sample under examination constituted of few-layer graphene [31]. The disorder-related D peak at ca. 1,350 cm^{-1} is present also in the pristine graphite powder, but its intensity is higher for graphene; this finding is in agreement with what reported in the literature in those cases in which graphene was produced by sonication of graphite and can be attributed to the new edges produced during the sonication process; the ultrasonic treatment causes the decrease in size of the flakes compared to the original graphite, with a consequent increase of the total edge length [32, 33].

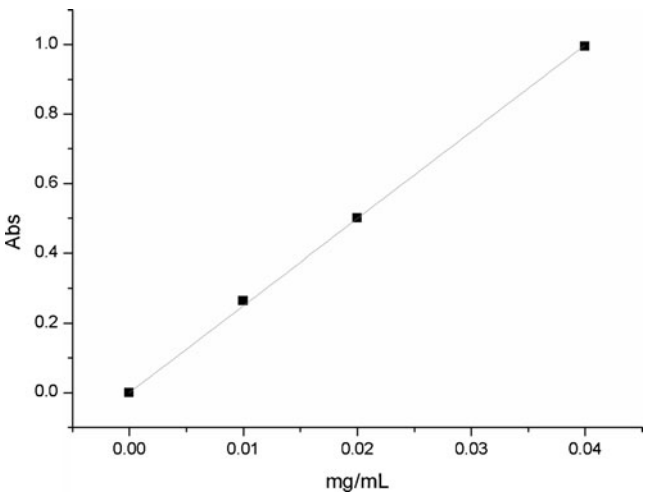

Fig. 1 Optical absorbance (660 nm) as a function of graphene concentration in DMF. The Lambert–Beer behavior is exhibited, with an absorption coefficient of 2,498 mL mg^{-1} m^{-1}

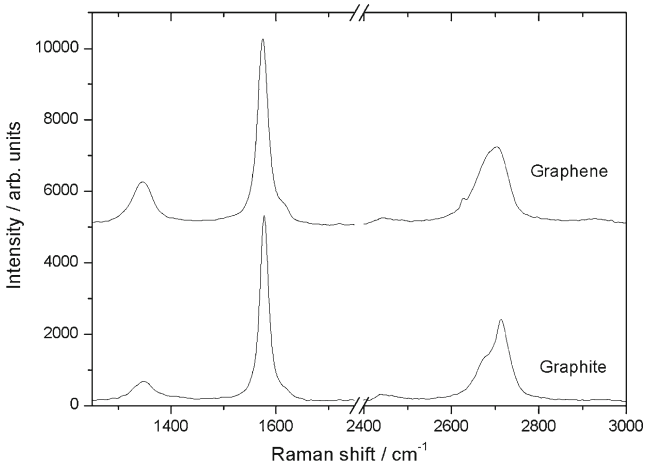

Fig. 2 Raman spectra of graphene obtained from DMF dispersion (*top line*) and graphite (*bottom line*)

TEM analysis is usually employed for the investigation of graphene dispersions [27, 29, 34]. As shown in Fig. 3, the micrographs evidence the formation of few-layer graphene. In particular, well-defined graphene sheets are clearly visible. It should be underlined that in all cases, graphite aggregates were not observed.

Characterization of graphene-based polymer nanocomposites

Swelling properties

First of all, the pH effect on the swelling behavior of hydrogels was studied, by varying the pH values from 3 to 12 and keeping the ionic force constant to 0.1. However, the obtained data are not reported here because the polymers were found to be more sensitive to the ionic force in comparison to pH and because, at this degree of ionic force, they are extremely deswollen; as a consequence, the pH influence is not well observable, and the trend cannot be rationalized. For such a reason, we focused on the influence of ionic strength and electrical field on SR%. In addition, the influence of graphene on these properties was investigated, in terms of emphasis or reduction of the SR% as a function of these two stimuli.

Various experiments were performed, in which only one of the above parameters was varied at once, while the others were kept constant.

The influence of ionic strength on SR% was studied by keeping the pH value constant and equal to 3, which is the natural pH of the aqueous medium resulting from the immersion of the hydrogels. For this experiment, two different salts were used—KNO_3 and $Ca(NO_3)_2$. They were chosen in order to investigate the different effects of a mono- or bivalent cation on the hydrogel swelling properties.

By using KNO_3, the ionic strength was varied from 0 to 0.1. The SR% decreases as the ionic strength increases, as shown well in Fig. 4.

The swelling behavior mainly depends on the diffusion of the ions and the fluid. By adding salt, a gap in the ionic concentration is created between the interior hydrogel and the external solution. The osmotic pressure due to the ionic concentration gap drives the ions to move from the solution into the hydrogel, in order to eliminate this concentration difference and to reach a dynamic equilibrium. This is achieved when the driving force is balanced by the elastic one; in consequence, the hydrogel shrinks [35].

The introduction of graphene within the hydrogel matrix does not influence the shrinking of hydrogels with increasing the ionic strength but allows the materials swelling more than the filler-free hydrogel, for each ionic strength value. This finding is in agreement with what already reported by us in the case of some thermoresponsive polymer hydrogels and might be attributed to the presence of graphene sheets that separate close macromolecular chains, thus reducing the cross-linking extent [18, 26].

Since a bivalent cation as Ca^{2+} can complex the hydrogel stronger than what K^+ can do, by using a solution of $Ca(NO_3)_2$, the hydrogels deswell more as the salt content raised; for such a reason, the influence of graphene on SR% is less pronounced (Fig. 5), and the samples had approximately the same swelling capacities regardless of the graphene content.

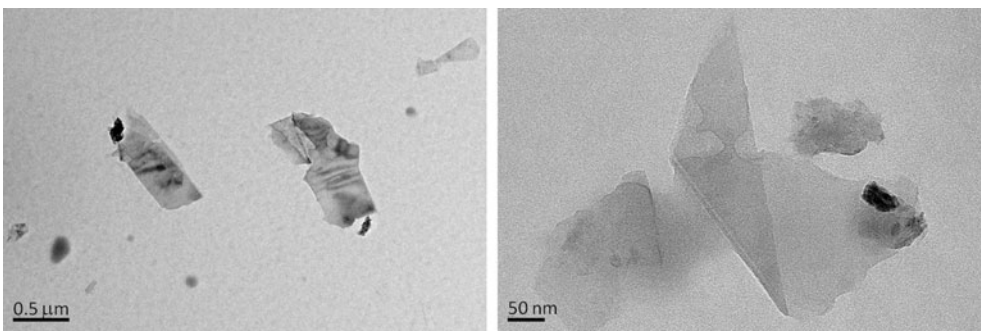

Fig. 3 TEM images of some graphene sheets (from the stock DMF/graphene dispersion diluted 1:10).

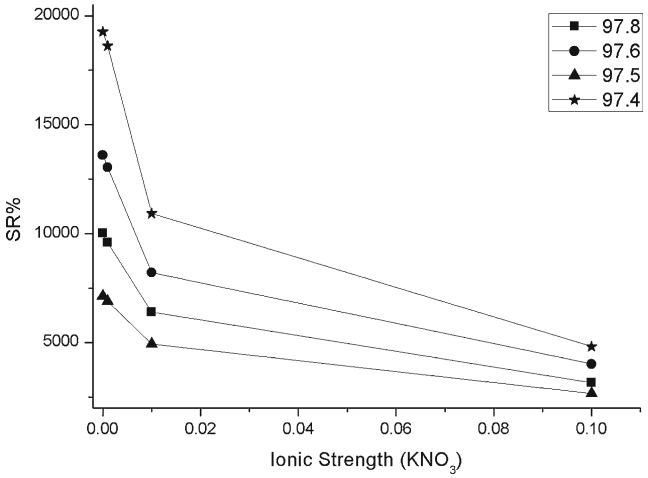

Fig. 4 SR% as a function of ionic strength for different graphene amounts (KNO_3 solution, sample 97.8=0 wt% of graphene, sample 97.6=0.01 wt% of graphene, sample 97.5=0.02 wt% of graphene, sample 97.4=0.06 wt% of graphene)

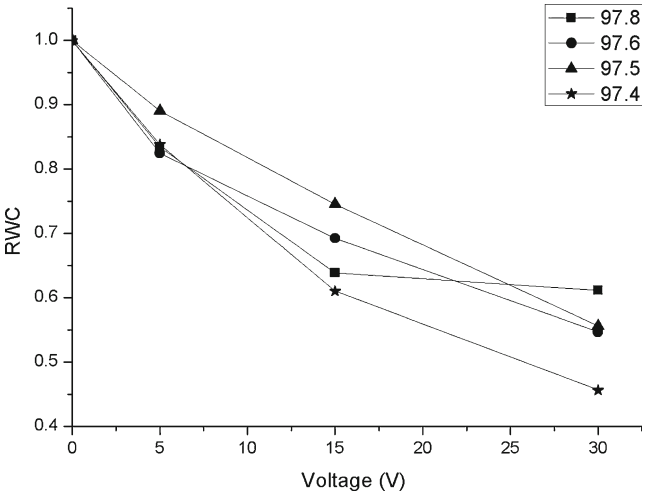

Fig. 6 RWC of hydrogels as a function of the voltage applied for different graphene amounts (sample 97.8=0 wt% of graphene, sample 97.6=0.01 wt% of graphene, sample 97.5=0.02 wt% of graphene, sample 97.4=0.06 wt% of graphene)

The pAMPSA hydrogels exhibit a variation of their size in response to a variation of an external electrical field. This type of behavior is due to a migration of the cations present inside the hydrogel toward the cathode, thus resulting in a partial shielding of the sulfonate group, which causes the decrease of gel hydration [1]. So, the hydrogels deswell with increasing the applied voltage (from 5 to 30 V) (Fig. 6). The RWC of the hydrogels was calculated by using Eq. (2).

As reported in the literature for polyelectrolyte hydrogels, the extent of deswelling increases with the magnitude of the electric field but is not linearly proportional to it; in particular, the behavior is characterized by an asymptotic trend for higher voltages [36]. Indeed, at the regimes, when gels are deswollen to a certain extent, their resistivity to the passage of a charge increases as the content of "free" water decreases. Subsequently, a smaller amount of a charge passes through the gel whose response is proportionally smaller.

In particular, according to the above statement, at higher voltages, the response magnitude of the filler-free sample tails off. At variance, the deswelling behavior of the nanocomposite hydrogels studied in the present work is different. Indeed, graphene influences this behavior—the filler-free sample (97.8) deswells as the applied voltage increases, up to 15 V. This fact indicates that the equilibrium swelling capability of this sample is exhibited at 15 V. At

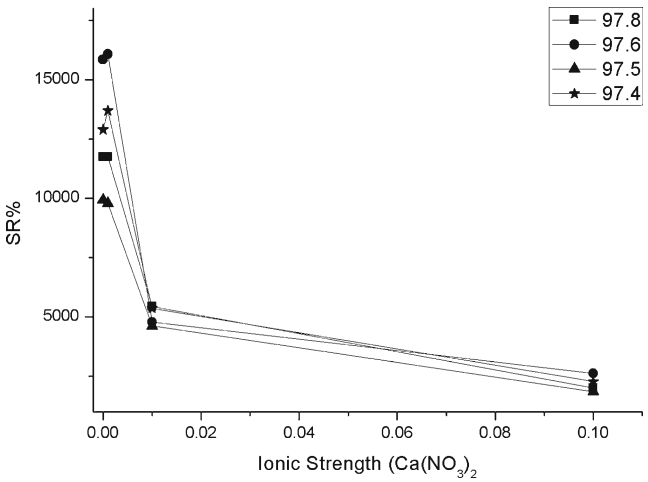

Fig. 5 SR% as a function of ionic strength for different graphene amounts ($Ca(NO_3)_2$ solution, sample 97.8=0 wt% of graphene, sample 97.6=0.01 wt% of graphene, sample 97.5=0.02 wt% of graphene, sample 97.4=0.06 wt% of graphene)

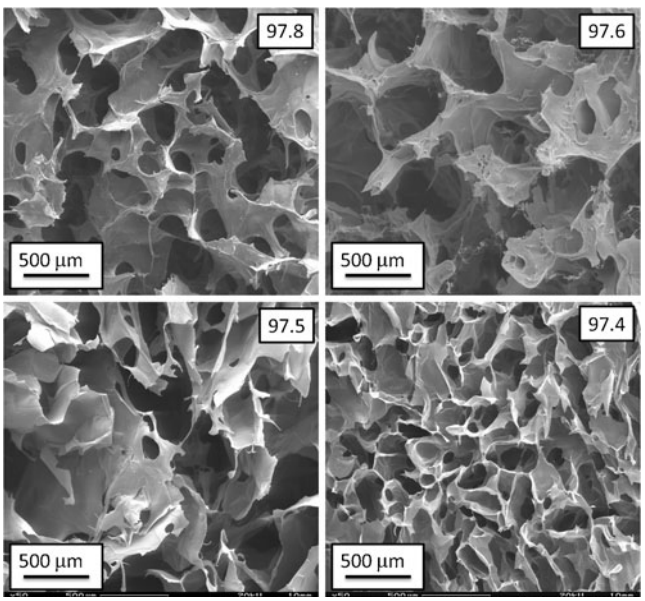

Fig. 7 Micrographs of hydrogel samples (sample 97.8=0 wt% of graphene, sample 97.6=0.01 wt% of graphene, sample 97.5=0.02 wt% of graphene, sample 97.4=0.06 wt% of graphene)

variance, the other samples, which contain graphene in different amounts, continue to deswell by an increasing voltage, at least up to the limit of 30 V used in our experiments.

Morphological analysis

In order to investigate the morphology of the hydrogels, SEM analysis was performed. In particular, no differences among samples containing graphene and filler-free samples were found; the hydrogel nanocomposites having different amounts of graphene are characterized by the typical hydrogel porous morphology, consisting of a spongy structure. All hydrogels prepared in the present work are characterized by inhomogeneous morphology independent of the graphene amount, with small pores having dimensions smaller than 250 μm, together with others that are larger than 500 mm (Fig. 7).

Conclusion

The synthesis of stimuli-responsive materials is one of the most innovative challenges in materials science. Namely, polymer hydrogels that respond to a variation of external conditions, such as temperature, pH, ionic strength, or electrical or magnetic fields, have a potential in many advanced applications.

In this work, polymeric nanocomposite hydrogels of pAMPSA-containing graphene were synthesized. It was found that they are responsive to variations of both ionic strength and electrical field, thus changing their swelling capability in aqueous solutions. In particular, the introduction of graphene in the hydrogel matrix increased the SR% of these materials and influenced its variation in response to the application of the stimuli.

As a matter of fact, by increasing the ionic strength of the solution in which they are immersed, they deswell. Moreover, the use of a Ca^{2+} instead of a K^{+} resulted in an increase of deswelling, which might be attributed to the larger coordinating capability of the bivalent cation as compared with the monovalent one and to the consequent different extents of non-covalent cross-linking. Besides, the shrinking is larger for graphene-containing hydrogels as compared with the filler-free sample. An analogous behavior is in agreement with what we found in other thermo-responsive polymer hydrogels as a consequence of temperature increase [18, 26]; actually, the larger is the graphene amount, the larger is the SR%. We think that it might be mainly due to an ineffective cross-linking among macromolecular chains that are separated by graphene sheets.

Furthermore, the polymer hydrogels studied here exhibited a response to the application of an electrical field. Namely, they contracted in different ways, depending on the graphene content and the applied voltage. It is noteworthy that the hydrogel sample that does not contain graphene exhibits an equilibrium swelling capability at 15 V, while the other samples, which contain different amounts of graphene, continue to deswell as voltage raises (up to 30 V, the highest voltage used in our experiments). These findings suggest that the neat hydrogel behaves as the typical dielectric materials do [37], while those that contain graphene are characterized by a completely different behavior.

Acknowledgments The authors thank the GEMPPO at the IEM-CSIC for allowing the use of the TEM. This work was partially supported by the Italian Ministry of University and Research.

References

1. Kim SJ, Lee CK, Kim SI (2004) Electrical/pH responsive properties of poly(2-acrylamido-2-methylpropane sulfonic acid)/hyaluronic acid hydrogels. J Appl Pol Sci 92:1731–1736
2. Gil ES, Hudson SM (2004) Stimuli-responsive polymers and their bioconjugates. Prog Polym Sci 29:1173–1222
3. Melekaslan D, Okay O (2000) Swelling of strong polyelectrolyte hydrogels in polymer solutions: effect of ion pair formation on the polymer collapse. Polymer 41:5737–5747
4. Otake M, Kayami Y, Inaba M, Inoue H (2002) Motion design of a starfish-shaped gel robot made of electro-active polymer gel. Robot Auton Syst 40:185–191
5. Kabiri K, Zohuriaan-Mehr MJ, Mirzadeh H, Kheirabadi M (2010) Solvent-, ion- and pH-specific swelling of poly(2-acrylamido-2-methylpropane sulfonic acid) superabsorbing gels. J Polym Res 17(203):212
6. Durmaz S, Okay O (2000) Acrylamide/2-acrylamido-2-methyl propane sulfonic acid sodium salt-based hydrogels: synthesis and characterization. Polymer 41:3693–3704
7. Ozmen MM, Okay O (2005) Superfast responsive ionic hydrogels with controllable pore size. Polymer 46:8119–8127
8. Wang KH, Choi MH, Koo CM, Choi YS, Chung IJ (2001) Synthesis and characterization of maleated polyethylene/clay nanocomposites. Polymer 42:9819–9826
9. Cavus S, Gurdag G (2009) Noncompetitive removal of heavy metal ions from aqueous solutions by poly[2-(acrylamido)-2-methyl-1-propanesulfonic acid-co-itaconic acid] hydrogel. Ind Eng Chem Res 48:2652–2658
10. Kajiwara K, Ross-Murphy SB (1992) Synthetic gels on the move. Nature 355:208–209
11. El-Hag AA, Abd El Rehim HA, Hegazy EA, Ghobashy MM (2006) Synthesis and electrical response of acrylic acid/vinyl sulfonic acid hydrogels prepared by γ-irradiation. Radiat Phys Chem 75:1041–1046
12. Yoshida R, Sakai K, Okano T, Sakurai Y (1993) Modern hydrogel delivery systems. Adv Drug Deliv Rev 11:85–108
13. Sawahata K, Hara M, Yasunaga H, Osada Y (1990) Electrically controlled drug delivery system using polyelectrolyte gels. J Control Release 14:253–262
14. Kwon IC, Bae YH, Okano T, Kim SW (1991) Drug release from electric current sensitive hydrogels. J Control Release 17:149–156
15. Kabiri K, Mirzade H, Zohuriaan-Meh MJ, Dalir M (2009) Chitosan-modified nanoclay–poly(AMPS) nanocomposite hydrogels with improved gel strength. Polym Int 58:1252–1259

16. Haraguchi K, Farnworth R, Ohbayashi A, Takehisa T (2003) Compositional effects on mechanical properties of nanocomposite hydrogels composed of poly (N, N-dimethylacrylamide) and clay. Macromolecules 36:5732–5741
17. Alzari V, Mariani A, Monticelli O, Valentini L, Nuvoli D, Piccinini M, Scognamillo S, Bittolo Bon S, Illescas J (2010) Stimuli-responsive polymer hydrogels containing partially exfoliated graphite. J. Polym Sci Par A: Pol Chem 48:5375–5381
18. Alzari V, Nuvoli D, Scognamillo S, Piccinini M, Gioffredi E, Malucelli G, Marceddu S, Sechi M, Sanna V, Mariani A (2011) Graphene-containing nanocomposite hydrogels of poly (*N*-isopropylacrylamide) prepared by frontal polymerization. J Mater Chem 21:8727–8733
19. Balandin AA, Ghosh S, Bao W, Calizo I, Teweldebrhan D, Miao F, Lau CN (2008) Superior thermal conductivity of single-layer graphene. Nano Lett 8:902–907
20. Bolotin KI, Sikes KJ, Jiang Z, Klima M, Fudenberg G, Hone J, Kim P, Stormer HL (2008) Ultrahigh electron mobility in suspended graphene. Solid State Commun 146:351–355
21. Stoller MD, Park S, Zhu Y, An J, Ruoff RS (2008) Graphene-based ultracapacitors. Nano Lett 8:3498–3502
22. Lee C, Wei X, Kysar JW, Hone J (2008) Measurement of the elastic properties and intrinsic strength of monolayer graphene. Science 321:385–388
23. Nuvoli D, Valentini L, Alzari V, Scognamillo S, Bittolo Bon S, Piccinini M, Illescas J, Mariani A (2011) High concentration few-layer graphene sheets obtained by liquid phase exfoliation of graphite in ionic liquid. J Mater Chem 21(3428):3431
24. Scognamillo S, Gioffredi E, Piccinini M, Lazzari M, Alzari V, Nuvoli D, Sanna R, Piga D, Malucelli G, Mariani A (2012) Synthesis and characterization of nanocomposites of thermoplastic polyurethane with both graphene and graphene nanoribbon fillers. Polymer 53:4019–4024
25. Alzari V, Nuvoli D, Sanna R, Scognamillo S, Piccinini M, Kenny JM, Malucelli G, Mariani A (2011) In situ production of high filler content graphene-based polymer nanocomposites by reactive processing. J Mater Chem 21:16544–16549
26. Sanna R, Sanna D, Alzari V, Nuvoli D, Scognamillo S, Piccinini M, Lazzari M, Gioffredi E, Malucelli G, Mariani A (2012) Synthesis and characterization of graphene-containing thermoresponsive nanocomposite hydrogels of poly(*N*-vinylcaprolactam) prepared by frontal polymerization. J Polym Sci Part A: Pol Chem 50:4110–4118
27. Hernandez Y, Nicolosi V, Lotya M, Blighe FM, Sun ZY, De S, McGovern IT, Holland B, Byrne M, Gun'ko YK, Boland JJ, Niraj P, Duesberg G, Krishnamurthy S, Goodhue R, Hutchison J, Scardaci V, Ferrari AC, Coleman JN (2008) High-yield production of graphene by liquid-phase exfoliation of graphite. Nat Nanotechnol 3:563–568
28. Mariani A, Nuvoli D, Alzari V, Pini M (2008) Phosphonium-based ionic liquids as a new class of radical initiators and their use in gas-free frontal polymerization. Macromolecules 41:5191–5196
29. Lotya M, Hernandez Y, King PJ, Smith RJ, Nicolosi V, Karlsson LS, Blighe FM, De S, Wang Z, McGovern IT, Duesberg GS, Coleman JN (2009) Exfoliation of graphite in surfactant/water solutions. J Am Chem Soc 131:3611–3620
30. Ferrari AC, Meyer JC, Scardaci V, Casiraghi C, Lazzeri M, Mauri F, Piscanec S, Jiang D, Novoselov KS, Roth S, Geim AK (2006) The Raman fingerprint of graphene. Phys Rev Lett 97(187401):1–4
31. Ferrari AC (2007) Raman spectroscopy of graphene and graphite: disorder, electron–phonon coupling, doping and nonadiabatic effects. Solid State Commun 143:47–57
32. Lotya M, King PJ, Khan U, De S, Coleman JN (2010) High-concentration, surfactant-stabilized graphene dispersions. ACS Nano 4:3155–62
33. Casiraghi C, Hartschuh A, Qian H, Piscanec S, Georgi C, Fasoli A, Novoselov KS, Basko DM, Ferrari AC (2009) Raman spectroscopy of graphene edges. Nano Lett 9:1433–41
34. Khan U, O'Neill A, Lotya M, De S, Coleman JN (2010) High-concentration solvent exfoliation of graphene. Small 6(7):864–871
35. Lai F, Li H (2010) Transient modeling for kinetic swelling/deswelling of the ionic-strength-sensitive hydrogel. Eur Phys J E 31:269–274
36. Murdan S (2003) Electro-responsive drug delivery from hydrogels. J Control Release 92:1–17
37. Wang Z, Nelson JK, Hillborg H, Zhao S, Schadler LS (2012) Graphene oxide filled nanocomposite with novel electrical and dielectric properties. Adv Mater 24:3134–3137